European Journal of Orthopaedic Surgery & Traumatology (2019) 29:967–973
https://doi.org/10.1007/s00590-019-02415-5

ORIGINAL ARTICLE • BIOMATERIAL - EXPERIMENTAL SURGERY

3D printing in experimental orthopaedic surgery: do it yourself

Irene I. López-Torres[1] · Pablo Sanz-Ruíz[1,2] · Victor E. León-Román[3] · Federico Navarro-García[4] · Rodrigo Priego-Sánchez[1] · Javier Vaquero-Martín[1,2]

Received: 12 December 2018 / Accepted: 5 March 2019 / Published online: 12 March 2019

Abstract

Introduction Periprosthetic infection is considered an increasing incidence pathology whose therapeutic strategies can be defined as unsatisfactory. Currently, animal models are employed to study its physiopathology and strategic therapies, but non-species-specific materials are implanted as foreign bodies. The use of these implants implies intrinsic instability, which hinders the development of a biofilm on their surfaces and complicates the post-operative recovery of the animal. The objective of the present study is the design of a species-specific implant for the New Zealand white (NZW) rabbit by means of 3D printing.

Materials and methods A CT scan of the knee of a NZW rabbit was performed, and the tibial surface was reconstructed in order to fabricate a species-specific tibial plateau using Horos® and Autodesk® Meshmixer™ software. This implant was inserted in fifteen NZW rabbits, and the assessment of its stability was based on the position of the limb at rest and the animal weight-bearing capacity. Biofilm formation on the surface was demonstrated by crystal violet staining.

Results A 1.81 cm × 1 cm × 1.24 cm stainless steel implant was designed. It consisted of a 4-mm-thick tibial plate with a rough surface and an eccentric metaphyseal anchoring. All of the animals exhibited hyperflexion of the operated limb immediately post-operative, and 100% could apply full weight bearing from day 5 after surgery.

Conclusions The species-specific design of implants in experimental surgery encourages rapid recovery of the animal and the development of a biofilm on their surfaces, making them ideal for the study of the physiopathology and for establishing possible therapeutic targets for prosthetic infection.

Keywords Periprosthetic joint infection · Animal model · Implant · 3D printing

Introduction

Infection following arthroplasty in orthopaedic surgery is a devastating complication whose presence can result in a significant functional loss of the affected limb and in a considerable risk of systemic complications. The increase in life expectancy of the population and the rising functional demands of young patients make periprosthetic infection (PJI) a growing pathology [1–3]. The treatment of PJI is based on systemic antibiotic therapy combined with different surgical strategies: irrigation and debridement, one-stage replacement and two-stage replacement. Depending on the series consulted, the success rates for each of these procedures vary between 10% and 75% for irrigation and debridement [4, 5], 86% and 100% for one-stage replacement [6, 7], and between 65% and 100% in two-stage replacement [8, 9]. Thus, PJI is considered a pathology of increasing incidence whose therapeutic strategies can be defined as unsatisfactory.

Currently, animal models are employed to study the pathogenesis of PJI and to choose potential therapeutic targets. As foreign bodies to promote the development of an infection, common clinical materials such as Kirschner wires or silicone metatarsophalangeal prostheses are used, but they are non-specific to the animal model. The use of non-specific implants complicates post-operative recovery

✉ Irene I. López-Torres
Irene.lopeztorres@gmail.com

1 Gregorio Marañón General Hospital, C/Doctor Esquerdo 46, Madrid, Spain

2 Surgery Department, Faculty of Medicine, Complutense University, Madrid, Spain

3 General Hospital of Villalba, Collado Villalba, Madrid, Spain

4 Department of microbiology, Faculty of Pharmacy, Complutense University of Madrid, Madrid, Spain

in the animal and can alter the recorded values of the defining parameters of infection and even result in the appearance of animal suffering signs that would inevitably lead to premature euthanasia and consequently increase the size of the sample needed to achieve the objective of the study. In addition, it is important to point out the great heterogeneity in the composition of the implants found in the bibliography, a factor of transcendental importance for the development of implant-associated infection [10].

The purpose of the present study is to create, by means of 3D technology, species-specific implants as tibial plateau substitutes in New Zealand White (NZW) rabbits which allow rapid recovery of animal movement, weight bearing and which facilitate the development of an infection on their surface.

Materials and methods

The experimental design of this study has been approved by the Committee for Animal Experimentation at the Complutense University of Madrid and by the Animal Protection Department of the Ministry of the Environment in the Community of Madrid (10/143903.9/17).

Implant design

For the 3D design of the tibial plateau, the right leg of a NZW rabbit with no musculoskeletal alterations and taken from a previously completed study, was used. Following euthanasia of the animal, a computerized axial tomography (CT scan) of the extremity was performed, which is the required first step in order to obtain DICOM images for the subsequent reconstruction.

The DICOM images from the CT scan were analysed using the Horos® (version 2.3.0 for Mac ©2015, Annapolis, MD, USA) image processing programme in order to create a three-dimensional surface of the rabbit knee [11]. An initial segmentation of the cortical surface of the proximal tibial metaphysis, defined as a "region of interest" (ROI), was performed. In order to optimize the focus on the areas of interest, a pixel value of 0 was applied to the regions not included in the ROI, and a pixel value of 1000 to the ROI selected in all the dynamic range of the image. Subsequently, 3D volumetric rendering of the highest quality images was performed with a resolution of 0.9 and a pixel value of 1000, the same as that assigned to the ROI. Following the volumetric reconstruction of the rabbit knee, the Autodesk® Meshmixer™ (version 3.1.373 for Mac ©2017, Autodesk, Inc. San Rafael, CA, USA) was employed to fabricate the tibial insert. Firstly, the proximal tibial metaphysis was separated from the lateral sesamoid and the fibula [12, 13]. The design of a 4-mm-thick tibial plate and the metaphyseal anchoring was carried out using the rough contour of the tibial surface as a template. The definitive insert was made of stainless steel. The reconstruction process of the rabbit tibia can be seen in Fig. 1.

The main problem encountered when designing the metaphyseal anchoring of the tibial insert was the small size of the medullary cavity (Fig. 2). The maximum anterior–posterior

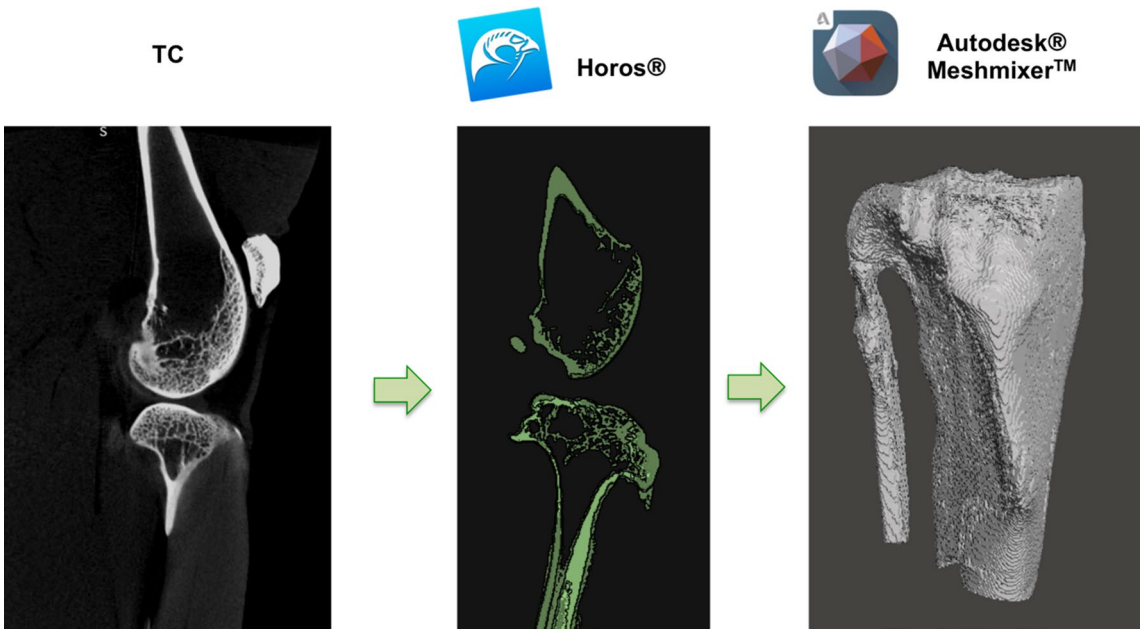

Fig. 1 Reconstruction process of the rabbit tibial plateau employing CT DICOM images (left), ROIs definition (centre) with Horos® and reconstruction of the 3D tibial plateau surface (right) with Autodesk® Meshmixer™

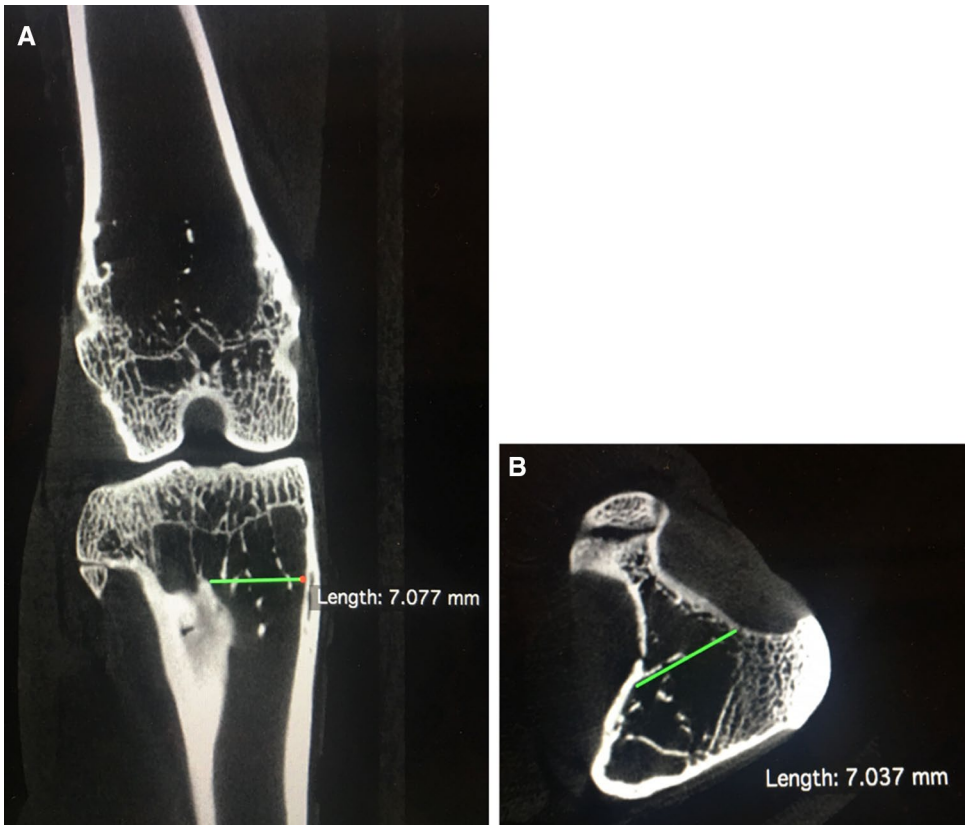

Fig. 2 CT images of the rabbit knee. **a** Coronal cut; **b** axial cut

diameter measured with the CT scan was 0.7 cm, and the maximum medial–lateral diameter was 0.7 cm. In addition, the diaphyseal canal of the tibia in these animals is centred with respect to the proximal articular surface, requiring the "rod" to be narrow and eccentric.

Surgical technique and assessment of implant stability

Sterilization of the fabricated metal implants was performed by moist heat in an autoclave at 134° and 2 atmospheres for 10 min, and these were then tested for stability in the experimental animals. Fifteen female NZW rabbits (Granja San Bernardo) weighing between 3 and 3.5 kilos were employed. Anaesthetic induction was achieved with 1.5 mL of ketamine (50 mg/kg) and 1.5 mL of xylazine (10 mg/kg), applied intramuscularly. As analgesic, meloxicam (1 mg/kg/day) was injected subcutaneously immediately post-operative and for the first four post-operative days.

To position the implant in the knee, a medial parapatellar approach, analogous to that common in clinical practice, was chosen. Both menisci and the anterior cruciate ligament were cut. A 4-mm resection of the tibial plateau was performed, and the medullary canal was prepared using a gouge. After checking the stability of the definitive implant, it was cemented without antibiotics (Palacos® R, Heraeus, Hanau, Germany).

Implant stability was assessed by monitoring two parameters: the position of the extremity at rest and its mobility during animal movement. Maintenance of hyperflexion of the knee was considered normal, and any other position of the limb was viewed as abnormal and as a sign of implant instability. In order to evaluate animal mobility, immediately following surgery and for 7 days thereafter, food was placed at the opposite end of the cage where the rabbit was located. An independent observer registered the mobility of the rabbits by awarding 1 point for non-weight bearing, 2 points for partial weight bearing, and 3 points for full weight bearing. Full weight bearing was defined as complete support on the extremity in 100% of the jumps made by the rabbits towards the food, non-weight bearing as complete lack of support, and partial weight bearing as any intermediate behaviour.

Evidence of biofilm formation in vitro

To demonstrate the ability of the insert to form a biofilm, the ATCC 29213 strain of *Staphylococcus aureus* was selected and a liquid culture (RPMI enriched with 0.2% glucose) of 5×10^6 CFU of the aforementioned bacteria was incubated at 37° with 5% CO_2 for 72 h. A change in the colour of the medium from rose to yellow was confirmed, in line with

the change in pH produced by microorganism growth. Two stainless steel tibial inserts were introduced in the culture to demonstrate bacterial growth on their surfaces and were incubated for 7 days [14].

Results

The implant designed was a one-piece, 4-mm-thick tibial plate with a rough surface, analogous to the tibial plateau of the rabbit. Initially, a tubular anchor system approximately 2 cm long was designed, but in 3D printing tests on polylactic acid the anchor system was broken. To avoid this problem, in order to control any implant rotation in the leg of the animal and to reduce the possibility of periprosthetic intraoperative fracture we modified the design using as anchoring system an eccentric stem in the shape of an inverted Gauss bell with smooth borders. The definitive size of the implant was 1.81 cm wide, 1 cm high, and 1.24 cm deep. This definitive version can be seen in Fig. 3.

All animals recovered from surgery without incident, and no peri-implant fractures occurred during the surgery. Hyperflexion of the affected member occurred in all of the rabbits immediately after surgery, and this was interpreted as normal. Follow-up results of animal mobility appear in Table 1. Every single rabbit exhibited partial weight bearing from day two, and all could apply full weight bearing on the extremity from day 5 post-operative and after the termination of the analgesic protocol. None of the animals showed the suffering signs that might have led to early euthanasia.

After 1 week incubation in the *Staphylococcus aureus* ATCC 29213® medium, the two stainless steel, rough-surface implants were stained with crystal violet to evidence the presence of a biofilm on their surfaces. The positive stain which was obtained from both implants can be seen in Fig. 4.

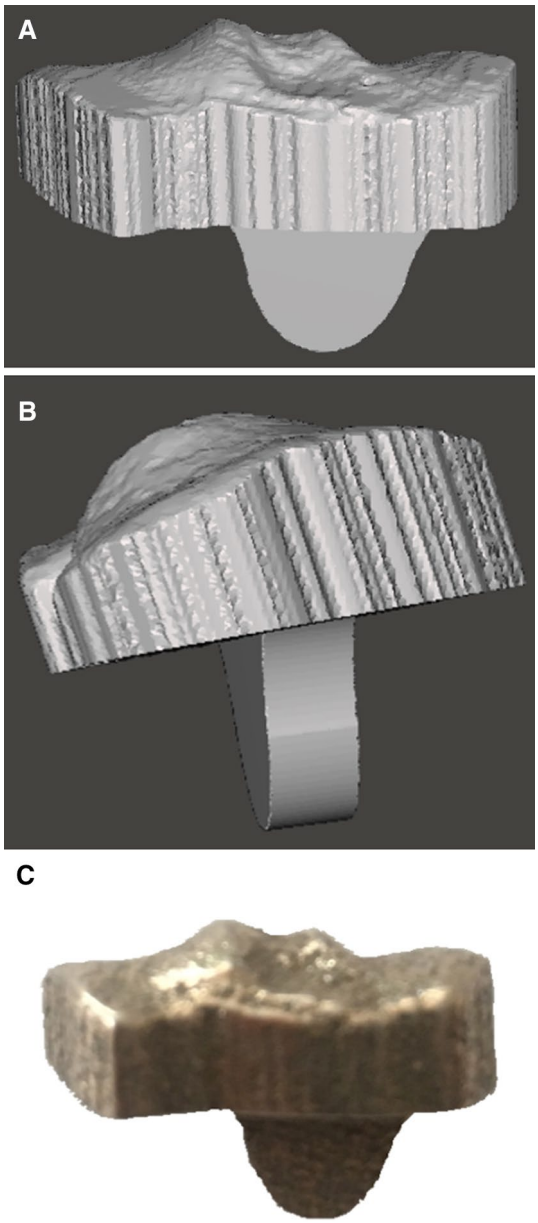

Fig. 3 Implant design. **a** Anteroposterior, **b** lateral view, and **c** stainless steel 3D printing

Discussion

The incorporation of 3D printing technology in the field of orthopaedic surgery has resulted in a radical change in clinical practice. It allows the design of patient-specific implants or templates, which has not only increased precision in procedures, but has also been shown to shorten surgery time and has consequently reduced complications. In addition, the ready availability of the materials and software required for the fabrication of these pieces has enabled the "Do it yourself" concept to reach the orthopaedic surgeon. This has in turn facilitated the custom design of material, not only for the patient, but also for the surgeon [12, 15, 16].

In the field of experimental surgery, 3D printing has been used to create molecular matrices (bone morphogenetic proteins and growth factors, among others) and mesenchymal, chondrocyte, and platelet cells, but its application in the design of implants is yet to be developed [17]. A great variety of implants employed to induce osteoarticular infections in animal models can be found, and to a large extent these are modifications of instruments used in common clinical practice, such as cannulated screws with cement injection, cemented or uncemented Kirschner wires, and even metatarsophalangeal silicone implants. Ofluoglu et al. [18] utilized titanium screws without cement augmentation to induce thoracic vertebrae infections; Clasper et al. [19] employed external 4 mm pins as intramedullary fixation devices, and

Table 1 Record of weight-bearing capacity of the limb

	Day 1	Day 2	Day 3	Day 4	Day 5	Day 6	Day 7
Non-weight bearing	8 (53.5%)	4 (26.7%)	2 (13.3%)	1 (6.7%)	0	0	0
Partial weight bearing	7 (46.7%)	10 (66.7%)	6 (40%)	8 (53.3%)	5 (33.3%)	0	0
Full weight bearing	0	1 (6.7%)	7 (46.7%)	6 (40%)	10 (66.7%)	100%	100%

Fig. 4 Evidence of biofilm formation by crystal violet staining 1 week after incubation with *S. aureus*

Belmatoug et al. [20] replaced the proximal tibial metaphyses of NZW rabbits with metatarsophalangeal silicone implants. The main disadvantage of these last two studies is that they required the assessment of implant-related complications by magnetic resonance imaging.

Another drawback of all of these studies is that the implants used are not designed *ex professo* for the animal in question, and this can lead to size or shape-related problems, which can in turn result in implant dislocation, peri-implant fractures, and osteochondral lesions. The host-implant discrepancy can also cause insert instability and unstable fixation of the bone. This has been shown to produce shearing forces that alter biofilm strength and density, which is undesirable when attempting to develop a clinically representative PJI model [21].

Carli et al. [22] published the only existing article we are aware of on the application of 3D design and printing in experimental orthopaedic surgery implants. In this report, a species-specific implant was fabricated to replace the proximal tibial in mice which consisted of a central stem and a flat articular surface. In our opinion, this design could restrict movement of the animal's limb and be a source of pain, especially if we consider the evident incompatibility of a totally flat tibial implant with curved femoral condyles. For this reason, in our study, we opted for a design of the tibial component which reproduced the anatomical shape of the tibial articular surface of the rabbit as faithfully as possible. This way, a highly suitable implant was fabricated which facilitated rapid post-operative functional recovery of the animal and provided a more physiological weight distribution.

The other factor to be considered in the design of an adequate implant to reproduce periprosthetic infection is its composition (alloying, surface characteristics, and porosity) [10, 23], bearing in mind that bacterial adhesion and biofilm creation are complex processes directly influenced by composition and implant loads. Many studies have shown a greater bacterial affinity for stainless steel implants, as opposed to those made of titanium or tantalum [10]. This increased affinity also applies to rough-surface implants, in contrast with hydrophobic ones [10, 23]. A Chang et al. [24] study compared the affinity of *Staphylococcus epidermidis* for stainless steel and titanium, both in vitro and in vivo, and evidenced greater bacterial affinity for stainless steel. Arens et al. [25] assessed the infection rate on stainless steel and titanium plates in NZW rabbits after local injection of $4 \times 10^{3-5}$ CFU of *Staphylococcus aureus*. Significant statistical differences between the infection rate of both implants were reported ($p = 0.018$) with titanium showing 35% and stainless steel 75%. With regard to the behaviour of new metals such as tantalum, the number of re-assessments resulting from sepsis in 144 total hip replacement cases was analysed in a noteworthy study by Tokarski et al. [26]. The rate of septic loosening was compared on the basis of the composition of the acetabular component (tantalum or titanium) and

showed a 17.5% rate for titanium implants versus 3.1% for tantalum with $p = 0.006$.

Despite the available evidence, PJI models can be found in the literature with a composition which appears contrary to that previously recommended. This is the case of Poultsides et al. [27], in which intramedullary tantalum cylinders were used to develop a model of MRSA haematogenous infection. Helbig et al. [28] also worked against the principles of bacterial affinity by employing titanium cylinders as foreign bodies to develop MRSA femoral osteomyelitis in NZW rabbits. In this last case, neither the infection rate nor any type of microbiological analyses was reported.

Taking into account the advances made in the recent years in 3D printing, we do not need to choose between congruence and implant surface properties any more. We can design implants with high congruence and print them in almost any material. If the purpose of our study is to develop a prosthetic joint infection, both aspects must be taken into account because using an adequate material by which bacteria have great affinity in an implant with lack of stability means lost of animals and diminish the strength of the adherence of the biofilm structure in the surface of the implant. Consequently, in the present study, species-specific stainless steel implants with rough surfaces were designed by means of 3D printing technology, in order to ensure good articular congruence and stable fixation, which are ideal for the development of periprosthetic infection.

Conclusions

3D printing facilitates the design of species-specific implants which, when utilized in experimental surgery, lead to rapid weight-bearing recovery of the extremity post-operatively. A customized articular substitution model has been created that can reproduce the knee arthroplasty environment at an experimental level. This is of incalculable value for biomechanical research, for the development of new prosthetic designs, and even for the study of the pathology and possible treatments of implant-related infection.

Funding Funding was provided by Santander-UCM Research Grants (PR26/16) and Mutual Medica Foundation Research Grants (2017).

Compliance with ethical standards

Conflict of interest The authors declare that they have no conflict of interest.

References

1. Malizos KN (2017) Global forum: the burden of bone and joint infections: a growing demand for more resources. J Bone Joint Surg Am 99:e20. https://doi.org/10.2106/JBJS.16.00240
2. Parvizi J, Pawasarat IM, Azzam KA, Joshi A, Hansen EN, Bozic KJ (2010) Periprosthetic joint infection: the economic impact of methicillin-resistant infections. J Arthroplasty 25:103–107. https://doi.org/10.1016/j.arth.2010.04.011
3. Kurtz SM, Lau E, Watson H, Schmier JK, Parvizi J (2012) Economic burden of periprosthetic joint infection in the United States. J Arthroplasty 27:61–65. https://doi.org/10.1016/j.arth.2012.02.022
4. Lora-Tamayo J, Murillo O, Iribarren JA, Soriano A, Sanchez-Somolinos M, Baraia-Etxaburu JM, Rico A, Palomino J, Rodriguez-Pardo D, Horcajada JP, Benito N, Bahamonde A, Granados A, del Toro MD, Cobo J, Riera M, Ramos A, Jover-Saenz A, Ariza J, Infection RGftSoP (2013) A large multicenter study of methicillin-susceptible and methicillin-resistant *Staphylococcus aureus* prosthetic joint infections managed with implant retention. Clin Infect Dis 56:182–194. https://doi.org/10.1093/cid/cis746
5. Koyonos L, Zmistowski B, Della Valle CJ, Parvizi J (2011) Infection control rate of irrigation and debridement for periprosthetic joint infection. Clin Orthop Relat Res 469:3043–3048. https://doi.org/10.1007/s11999-011-1910-2
6. Jiranek WA, Waligora AC, Hess SR, Golladay GL (2015) Surgical treatment of prosthetic joint infections of the hip and knee: changing paradigms? J Arthroplasty 30:912–918. https://doi.org/10.1016/j.arth.2015.03.014
7. Garcia S, Soriano A, Esteban P, Almela M, Gallart X, Mensa J (2005) Usefulness of adding antibiotic to cement in one stage exchange of chronic infection in total hip arthroplasty. Med Clin (Barc) 125:138–139
8. Schindler M, Christofilopoulos P, Wyssa B, Belaieff W, Garzoni C, Bernard L, Lew D, Hoffmeyer P, Uckay I (2011) Poor performance of microbiological sampling in the prediction of recurrent arthroplasty infection. Int Orthop 35:647–654. https://doi.org/10.1007/s00264-010-1014-8
9. Anagnostakos K (2017) Therapeutic use of antibiotic-loaded bone cement in the treatment of hip and knee joint infections. J Bone Joint Infect 2:29–37. https://doi.org/10.7150/jbji.16067
10. Cordero J, Munuera L, Folgueira MD (1994) Influence of metal implants on infection. An experimental study in rabbits. J Bone Joint Surg Br 76:717–720
11. Fadero PE, Shah M (2014) Three dimensional (3D) modelling and surgical planning in trauma and orthopaedics. Surgeon 12:328–333. https://doi.org/10.1016/j.surge.2014.03.008
12. Arnal-Burro J, Perez-Mananes R, Gallo-Del-Valle E, Igualada-Blazquez C, Cuervas-Mons M, Vaquero-Martin J (2017) Three dimensional-printed patient-specific cutting guides for femoral varization osteotomy: do it yourself. Knee 24:1359–1368. https://doi.org/10.1016/j.knee.2017.04.016
13. Perez-Mananes R, Burro JA, Manaute JR, Rodriguez FC, Martin JV (2016) 3D surgical printing cutting guides for open-wedge high tibial osteotomy: do it yourself. J Knee Surg 29:690–695. https://doi.org/10.1055/s-0036-1572412
14. O'Toole GA (2011) Microtiter dish biofilm formation assay. J Vis Exp. https://doi.org/10.3791/2437
15. Auricchio F, Marconi S (2016) 3D printing: clinical applications in orthopaedics and traumatology. EFORT Open Rev 1:121–127. https://doi.org/10.1302/2058-5241.1.000012
16. Frame M, Leach W (2014) DIY 3D printing of custom orthopaedic implants: a proof of concept study. Surg Technol Int 24:314–317

17. Wang H, Wu G, Zhang J, Zhou K, Yin B, Su X, Qiu G, Yang G, Zhang X, Zhou G, Wu Z (2016) Osteogenic effect of controlled released rhBMP-2 in 3D printed porous hydroxyapatite scaffold. Colloids Surf B Biointerfaces 141:491–498. https://doi.org/10.1016/j.colsurfb.2016.02.007
18. Ofluoglu EA, Bulent E, Derya AM, Sancar BY, Akin G, Bekir T, Erhan E (2012) Efficiency of antibiotic-loaded polymethylmethacrylate rods for treatment of the implant-related infections in rat spine. J Spinal Disord Tech 25:E48–E52. https://doi.org/10.1097/BSD.0b013e3182425b93
19. Clasper JC, Stapley SA, Bowley DM, Kenward CE, Taylor V, Watkins PE (2001) Spread of infection, in an animal model, after intramedullary nailing of an infected external fixator pin track. J Orthop Res 19:155–159. https://doi.org/10.1016/S0736-0266(00)00023-1
20. Belmatoug N, Cremieux AC, Bleton R, Volk A, Saleh-Mghir A, Grossin M, Garry L, Carbon C (1996) A new model of experimental prosthetic joint infection due to methicillin-resistant *Staphylococcus aureus*: a microbiologic, histopathologic, and magnetic resonance imaging characterization. J Infect Dis 174:414–417
21. Liu Y, Tay JH (2001) Metabolic response of biofilm to shear stress in fixed-film culture. J Appl Microbiol 90:337–342
22. Carli AV, Bhimani S, Yang X, Shirley MB, de Mesy Bentley KL, Ross FP, Bostrom MP (2017) Quantification of peri-implant bacterial load and in vivo biofilm formation in an innovative, clinically representative mouse model of periprosthetic joint infection. J Bone Joint Surg Am 99:e25. https://doi.org/10.2106/JBJS.16.00815
23. Cordero J, Munuera L, Folgueira MD (1996) The influence of the chemical composition and surface of the implant on infection. Injury 27(Suppl 3):SC34–SC37
24. Chang CC, Merritt K (1994) Infection at the site of implanted materials with and without preadhered bacteria. J Orthop Res 12:526–531. https://doi.org/10.1002/jor.1100120409
25. Arens S, Schlegel U, Printzen G, Ziegler WJ, Perren SM, Hansis M (1996) Influence of materials for fixation implants on local infection. An experimental study of steel versus titanium DCP in rabbits. J Bone Joint Surg Br 78:647–651
26. Tokarski AT, Novack TA, Parvizi J (2015) Is tantalum protective against infection in revision total hip arthroplasty? Bone Joint J 97-B:45–49. https://doi.org/10.1302/0301-620x.97b1.34236
27. Poultsides LA, Papatheodorou LK, Karachalios TS, Khaldi L, Maniatis A, Petinaki E, Malizos KN (2008) Novel model for studying hematogenous infection in an experimental setting of implant-related infection by a community-acquired methicillin-resistant *S. aureus* strain. J Orthop Res 26:1355–1362. https://doi.org/10.1002/jor.20608
28. Helbig L, Simank HG, Lorenz H, Putz C, Wolfl C, Suda AJ, Moghaddam A, Schmidmaier G, Guehring T (2014) Establishment of a new methicillin resistant *Staphylococcus aureus* animal model of osteomyelitis. Int Orthop 38:891–897. https://doi.org/10.1007/s00264-013-2149-1